

## Experimental Investigations of the Effect of Reynolds Number on a Plane Jet

Ravinesh C Deo<sup>1</sup>, Jianchun Mi<sup>2</sup> and Graham J Nathan<sup>2</sup>

<sup>1</sup>Center for Remote Sensing and Spatial Information Sciences  
 School of Geography Planning and Architecture  
 The University of Queensland  
 Brisbane 4072 AUSTRALIA  
 Corresponding Author: [r.deo1@uq.edu.au](mailto:r.deo1@uq.edu.au)

<sup>2</sup>Turbulence, Energy and Combustion Group, School of Mechanical Engineering  
 The University of Adelaide, Adelaide, South Australia, 5005 AUSTRALIA

### Abstract

The effect of Reynolds number,  $Re = U_{o,c}H / \mu$ , where  $U_{o,c}$  is the nozzle exit centreline velocity,  $H$  is the slot-opening width and  $\mu$  is the kinematic viscosity of air) on the velocity field of a turbulent plane jet from a radially contoured nozzle of aspect ratio 60 is investigated. Measurements are conducted using a single wire anemometer over an axial distance of  $160H$ . The Reynolds number is varied between 1,500 and 16,500. Results show that the  $Re$  affects various flow properties such as the velocity decay rate, half-width and turbulence intensity. The significant dependence on  $Re$  of the mean flow field persists till  $Re = 16,500$ , while the  $Re$  effect on the turbulent properties becomes weaker above  $Re = 10,000$ . The present investigation also suggests that an increase in  $Re$  leads to a higher rate of mixing in the near field but a lower rate in the far field.

### Introduction

A true plane jet issues from a rectangular nozzle of high aspect ratio,  $w/H$  (where  $w$  is the short side and  $H$  is the long side of the rectangular nozzle). The jet is confined within two parallel side walls, attached to the short sides of the nozzle. This configuration enables the jet to spread in the lateral ( $y$ ) direction only. Some applications of a plane jet include engineering environments, e.g. in propulsion units and lift-producing devices, Quinn [1], air curtains and some combustion applications.

It is well established experimentally that, at sufficiently high Reynolds number, the normalized mean velocity profiles and the spreading rates of a round jet are almost independent of Reynolds number (Panchapakesan and Lumley [1], Hussain et al. [3]). The visualizations of Mungal and Hollingsworth [4] for their jet at very high Reynolds number ( $Re \sim 2 \times 10^8$ ) showed that its spreading rates and normalized mean velocity profiles are close to those of a laminar jet. In contrast, at low Reynolds numbers, both the mean and turbulent flow fields depend significantly on  $Re$ . This is evident, from Oosthuizen [5] for round jet, measured at moderate  $Re$ . Likewise, both Lemieux and Oosthuizen [6] and Namar and Otugen [7], studied the effect of Reynolds number in a plane free jet, over the  $Re$  ranges of 700 – 4200 and 1000 – 7000, revealed that  $Re$  influenced the entire mixing field.

When Lofdahl et al. [8] investigated a plane wall jet, they found the jet spreading rates to remain variable even up to  $Re = 20,000$ . An investigation by Stanley et al [9] and Klein et al [10] at  $Re = 3,000$  and  $Re \sim 6,000$ , respectively, was conducted only in the near and transition fields ( $x/H \leq 15$  and  $x/H \leq 20$ ) even though Klein et al [10] claimed they covered the far field.

Clearly, wide range of different conditions makes it impossible to isolate the effect of Reynolds number from that of other variables. Hence conclusive quantitative data describing the  $Re$  dependence of a plane jet is not available. To address this issue, we have carried out an experimental investigation into a plane jet at  $Re$  between 1,500 and  $Re = 16,500$ , using a radial

contraction nozzle with aspect ratio of  $w/H = 60$ , bounded by side walls, over a wider  $Re$ -range, and flow region up to  $x/H = 160$ .

### Experimental Details

The overall jet facility, shown in Figure 1, has been described in detail in Deo [11].

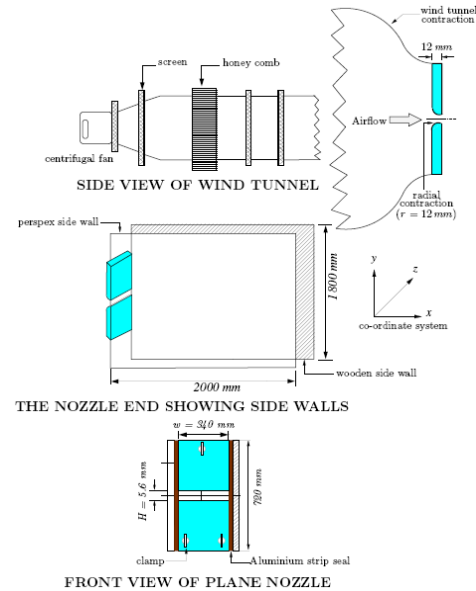


Figure 1: Schematic diagrams of the plane jet facility, showing the wind tunnel, plane nozzle arrangement and side-walls.

The present plane nozzle is referred to as a radial contraction nozzle  $r/H \approx 2.14$ , where  $r$  is the nozzle exit radius), to differentiate it from the smooth contraction nozzles used in most previous investigations (e.g. Gutmark and Wyngnanski [11], Namar and Otugen [7], Bradbury [13] and Antonia et al [14]). For a comprehensive description of the radially contoured nozzle, see Deo [11] and Deo et al [15]. A constant temperature hot-wire anemometer (CTA) was employed to undertake measurements. A copper plated tungsten single hot wire probe, length  $l_w \sim 1$  mm and diameter  $d_w \sim 5 \mu m$  was mounted parallel to the  $z$ -axis of the traverse. Hot wire calibration was performed in the jet potential core (turbulence intensity  $\sim 0.5\%$ ). Control of the jet Reynolds number,  $Re = U_{o,c}H / \mu$ , was achieved by varying the speed of the wind tunnel fan. The maximum achievable Reynolds number was 16,500, without reducing the nozzle aspect ratio. The range of Reynolds numbers was selected to be  $1,500 \leq Re \leq 16,500$ . The extent of measurements along the axial direction was  $0 \leq x/H \leq 160$ , to include the near, transition and far fields.

### Results and Discussion

Figure 2 shows the normalized profiles of mean velocity and turbulence intensity obtained at  $x \approx 0.5H$  for  $Re = 3,000, 10,000$  and  $16,500$ .

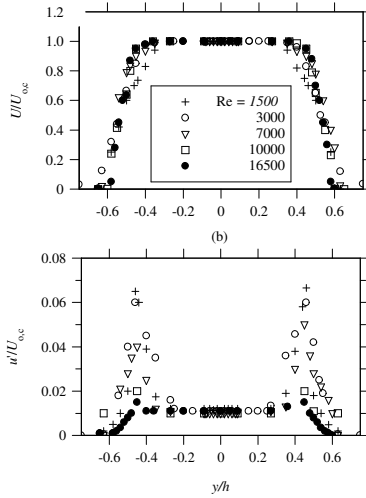


Figure 2: Lateral profiles of (a) normalized mean velocity and (b) turbulence intensity obtained at  $x/H \approx 0.5$ .

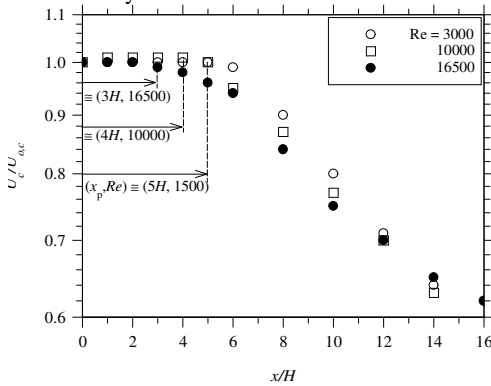


Figure 3 The near-field mean velocity variation along the centerline and potential core length for different  $Re$ .

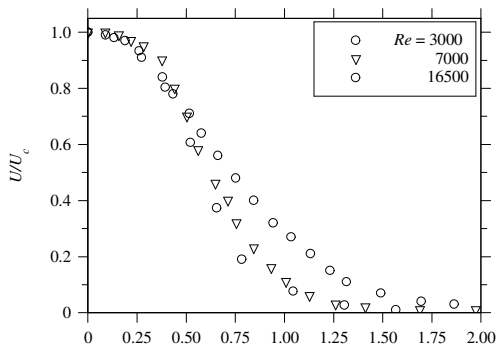


Figure 4: Lateral profiles of  $U/U_c$  at  $x/H = 5$ .

A dependence of the normalized exit velocity and turbulence intensity profiles on  $Re$  is noticeable. However, they become nearly identical when  $Re \approx 10,000$ . Dependence of exit velocity profiles on  $Re$  were also noted by Namar and Otugen [7] for their 'plane' jet without side walls, however, their velocity profiles did not become identical even at  $Re = 7,000$ . The present turbulence intensities in the central region ( $|y/H| \leq 0.3 - 0.4$ ) are below 1.0% for all  $Re$ . The peak values of turbulence intensity occur in the mixing layers and their magnitudes decrease as Reynolds number increases. Furthermore, over the range  $|y/H| \leq 0.30 - 0.4$ , the

mean velocity is uniform (i.e.  $U/U_{o,c} \sim 1$ ), indicating that the present radial contraction nozzle can produce a similar exit velocity profile to that from the conventional smooth contraction nozzle.

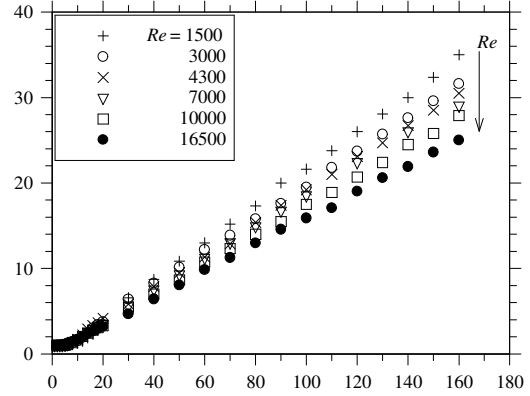


Figure 5: Centerline variation of the mean velocity decay.

Figure 3 presents the near-field mean velocity along the centerline. As demonstrated, the length ( $x_p$ ) of the potential core, where the mean velocity is approximately constant and equal to  $U_{o,c}$  is a function of  $Re$ . For example,  $x_p/H \approx 5$  for  $Re = 3,000$  and  $x_p/H \approx 3$  for  $Re = 16,500$ . Namely,  $x_p/H$  decreases with  $Re$ . Correspondingly, the jet spreads more rapidly for higher  $Re$ , which is verified by lateral profiles of  $U/U_c$  in Figure 4. These together imply that the relative entrainment, thus mixing, of the jet is enhanced by increasing the  $Re$  in the near field.

Investigation	Re	Decay		Spread	
		$K_u$	$x_{01}/H$	$K_v$	$x_{02}/H$
Jenkins & Goldschmidt [17]	14000	0.160	0.40	0.093	-8.20
Hitchman et al. [16]	7000	0.147	8.05	0.108	-1.94
Browne et al. [18]	7700	0.147	8.05	0.112	-1.94
Gutmark & Wygnanski [12]	30000	0.174	-0.7	0.099	-3.21

Table 1: A summary of plane jet decay and spreading of jets with side walls

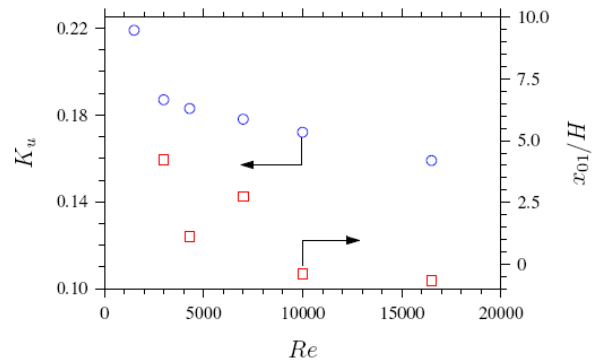


Figure 6: Dependence of  $K_u$  and  $x_{01}$  on  $Re_h$

The mean velocity decay is shown in Figure 4. The data conform to the well-known inverse square relationship expressed by

$$\left[ \frac{U_{o,c}}{U_c} \right]^2 = K_u \left[ \frac{x}{H} + \frac{x_{01}}{H} \right]$$

where  $K_u$  is the slope and  $x_{01}$  is the  $x$ -location of the virtual origin of the profiles.

Figure 5 demonstrates that the velocity decay rates for  $Re_h = 7,000$  and  $16,500$  agree well with Hitchman et al. [16] for  $Re = 7,000$  and Jenkins and Goldschmidt [17] for  $Re = 14,000$ ,

providing confidence in our measurements. Further, the velocity decay rate can be measured by the magnitudes of  $K_u$ .

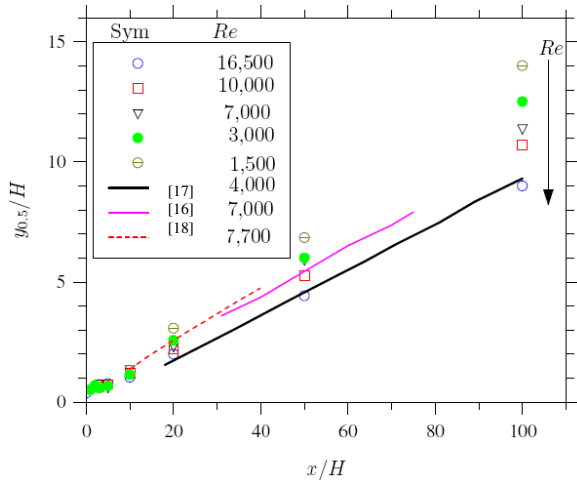


Figure 8: Dependence of  $K_y$  on the Re.

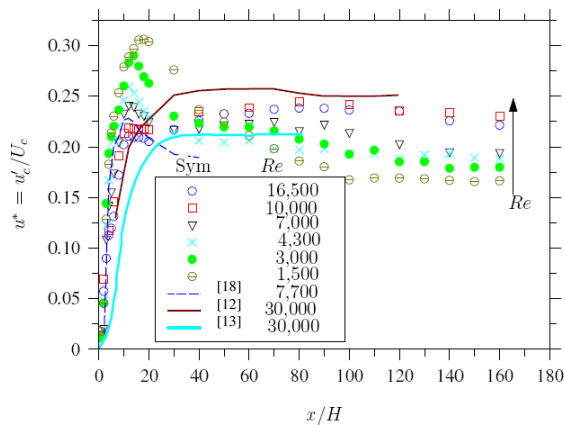


Figure 9: Evolutions of the centerline turbulence intensity.

Figure 6 shows the dependence of  $K_u$  on  $Re$ . As demonstrated,  $K_u$  decreases monotonically with an increase in  $Re$  and that  $K_u$  does not approach to an asymptotic value, even at to  $Re = 16,500$ . This suggests that the  $Re$  continues to affect the mean velocity field even at  $Re = 16,500$ . In addition, it appears from Figure 6 that the virtual origin  $x_{0I}$  is smaller at higher Reynolds number.

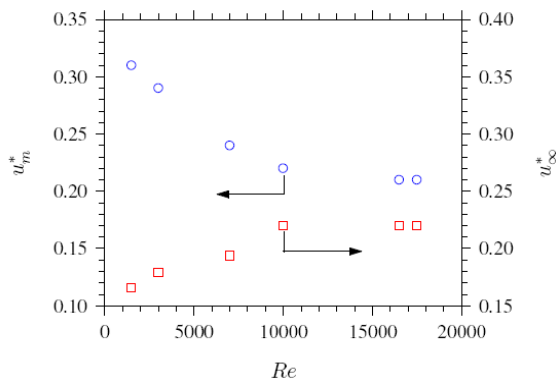


Figure 10: Reynolds number effect on  $u_m^*$  and  $u_\infty^*$ .

Figure 7 shows the stream wise variations of the velocity half-width  $y_{0.5}$  at different Reynolds numbers. Note that  $y_{0.5}$  is the lateral distance from the centerline at which the local mean

velocity is half the centerline value. The values of  $y_{0.5}$  were derived from the lateral velocity measurements (not presented here).

As expected, the data conform to the following far-field relation:

$$\frac{y_{0.5}}{h} = K_y \left[ \frac{x}{h} + \frac{x_{02}}{h} \right]$$

where constants  $K_y$  and  $x_{02}$  are determined by experiments.

When  $Re$  changes from 1,500 to 16,500, the half-width spreads out at different rates. This is better illustrated in Figure 8 by the  $Re$ -dependence of  $K_y$ , a measure of the spreading rate. Clearly, the spreading rate decreases with an increase in  $Re$  which is consistent with the trend in the decay of  $U_c$  (Fig. 5). This together proves that, different from the near-field case, the far-field entrainment rate is reduced by increasing  $Re$ .

Figure 9 shows the centerline turbulence intensities (normalized rms,  $u^* = u'_c/U_c$ ) for the different  $Re$  values. The development of  $u^*$  is similar to that of Browne et al. [13] for a plane jet ( $w/H = 20$  and  $Re = 7,700$ ). However, the near-field local maximum in the intensity ( $u_m^*$ ) is slightly different. Their local maximum occurs at  $x/H = 12$  and has a magnitude of 0.23 while ours for  $Re = 7,000$  occurs at  $x/H = 11$  and has a magnitude of 0.24. This difference could be due to the big difference in the aspect ratio (our  $w/H = 60$  versus  $w/H = 20$  in Browne et al. [18]). Thomas and Goldschmidt [19] found yet another value of the maximum for  $Re = 6,000$ , which occurs at  $x/H = 11$ , with a magnitude of 0.27. The discrepancies observed are likely due to differences in jet initial conditions, consistent with Mi et al. [20], that the occurrence of the pronounced local maximum in scalar intensity of a round jet depends upon exit conditions.

Further, as  $Re$  increases from 1,500 to 16,500, the magnitudes of  $u_m^*$  decreases from 0.31 to 0.22 (Fig. 10). The values of  $u_m^*$  are nearly identical for  $Re \geq 10,000$ . The occurrence of higher  $u_m^*$  for lower  $Re$  suggests that the underlying large-scale structures are initially more coherent and organized for low Reynolds numbers. In these cases, the intermittent incursion of induced low velocity ambient fluid across the jet produces higher fluctuation amplitudes and lower mean values of the local velocity, and thus higher relative turbulence intensities. When  $Re$  is increased, the underlying structures become more three-dimensional and less coherent, and consequently the magnitude of  $u_m^*$  is reduced. Figure 10 also indicates that  $u^*$  converges to a single curve for  $Re = 10,000$  and 16,500. It appears as well that in both cases  $u^*$  reaches an asymptotic value of  $u_\infty^* = 0.22$  at  $x/H > 60$ . However, for  $Re < 10,000$ , the intensity and its evolution trend are both strongly dependent on the  $Re$ . Over  $100 \leq x/H \leq 160$ ,  $u^*$  asymptotes to different values of  $u_\infty^*$  for different  $Re$  for  $Re < 10,000$ , see Fig. 10. Clearly,  $u_\infty^*$  increases with increasing  $Re$ .

## Conclusion

The measurements revealed that  $Re$  affect various flow properties (mean velocity decay rate, half-width and turbulence intensity). The dependence on  $Re$  of the mean flow field appears to persist at  $Re = 16,500$ , while the  $Re$  effect on the turbulent properties is eliminated above  $Re \approx 10,000$ . Our measurements also suggest that increasing  $Re$  leads the jet to mix its surroundings at a higher rate in the near field but less rapidly in the far field.

Specifically, the findings from present work are as follows.

- Our radially contoured nozzle, of  $r/H \approx 2.14$ , generates a quasi-top hat mean exit velocity profile. The uniform part of the profile widens as the  $Re$  increases. For  $Re \geq 10,000$ , the profiles become independent of  $Re$ .
- The length of jets' potential core decreases with  $Re$ . The jet decay and spread rates downstream of the potential core

decrease with increasing Re, and this trend persists even at Re = 16,500.

- The centerline turbulence intensity shows a local maximum in the near-field. Below Re = 10,000, its magnitude and axial location decrease as Re is increased.

## Acknowledgments

The authors acknowledge the support of ARC Discovery Grant, International Postgraduate Research Scholarship and Adelaide University Scholarship for supporting first author's PhD research on which this paper is based.

## References

- [1] Quinn W R. Development of a large-aspect ratio rectangular turbulent free jet. *AIAA Journal*, 32(3), 547-555, 1994.
- [2] Panchapakesan N R and Lumley J L. Turbulence measurements in axisymmetric jets of air and helium, part 1, air jet. *J. Fluid Mech.*, 246, 197-223, 1993.
- [3] Hussain H J, Capp S P , and George W K. Velocity measurements in a high Reynolds number momentum conserving axisymmetric turbulent jet. *J. Fluid Mech.*, 258, 31-75, 1994.
- [4] Mungal G and Hollingsworth D K. Organized motion in a high Reynolds number jet. *Phys. Fluids*, 1(10), 1615-1623, 1989.
- [5] Oosthuizen P H. An experimental study of low Reynolds number turbulent circular jet flow. volume 83-FE-36 of ASME Applied Mechanics, Bioengineering, and Fluids Engineering Conference, Houston/TX USA, June 20-22 1983.
- [6] Lemieux G P and Oosthuizen P H. Experimental study of behaviour of plane turbulent jets at low Reynolds numbers. *AIAA Journal*, pages 1845, 1846, 1985.
- [7] Namar I and Otugen M V. Velocity measurements in a plane turbulent air jet at moderate Reynolds numbers. *Exp. Fluids*, 6:387{399, 1988.
- [8] Lofdahl L, H Abrahamson, B Johansson and T Hadzianagnostakis. On the Reynolds number dependence of a plane two-dimensional wall-jet. *Doktorsavhandlingar vid Chalmers Tekniska Hogskol*, 1292, 8pp, 1997.
- [9] Stanley S A, Sarkar S, and Mellado J P. A study of the eld evolution and mixing in a planar turbulent jet using direct numerical simulations. *J. Fluid Mech.*, 450, 377-407, 2002.
- [10] Klein M, Sadiki A, and Janicka J. Investigation of the influence of the Reynolds number on a plane jet using direct numerical simulation. *Int. J. Heat and Fluid Flow*, 24, 785-794, 2003.
- [11] Deo R C. Experimental investigations of the influence of Reynolds number and boundary conditions on a plane air jet. Ph.D. thesis, School of Mechanical Engineering, The University of Adelaide, South Australia, ADT Program: <http://thesis.library.adelaide.edu.au/public/adt-UA20051025.054550/index.html>, (2005).
- [12] Gutmark E and Wygnanski I. The planar turbulent jet. *J. Fluid Mech.*, 73(3), 465-495, 1976.
- [13] Bradbury L J S. The structure of self-preserving turbulent plane jet. *J. Fluid Mech.*, 23, 31-64, 1965.
- [14] Antonia R A, Browne W B, Rajagopalan S , and Chambers A J . On organized motion of a turbulent plane jet. *J. Fluids Mech.*, 134, 49-66, 1983.
- [15] Deo R C, Mi, J and Nathan, G J. The influence of nozzle-exit geometric profile on statistical properties of a plane jet. *Experim. Therm. Fluid Sc.* Online doi: 10.1016/j.expthermflusci.2006.08.010, 32(2), 545-559
- [16] Hitchman G J, Strong A B, Slawson P R and Ray G . Turbulent plane jet with and without confining walls. *AIAA Journal*, 28(10), 1699-1700, 1990.
- [17] Jenkins P E and Goldschmidt V W. Mean temperature and velocity measurements in a plane turbulent jet. *Trans. ASME J.*, 95, 581-584, 1973.
- [18] Browne L W B, Antonia R A, Rajagopalan S and Chambers A J. Interaction region of a two-dimensional turbulent plane jet in still air. In *Structure of Complex Turbulent Shear Flows*, IUTAM Symposium, 411-419, 1982.
- [19] Thomas F O and Goldschmidt V W. Structural characteristics of a developing turbulent planar jet. *J. Fluid Mech.*, 163, 227-256, 1986.
- [20] Mi J, Nobes D and Nathan G J. Influence of exit conditions of round nozzles on the passive scalar field of a jet. *J. Fluid Mech.*, 432, 91-125, 2001.